Available online at www.eccomasproceedia.org
Eccomas Proceedia SMART (2023) 477-488

ECCOMAS
Proceedia

X ECCOMAS Thematic Conference on Smart Structures and Materials
SMART 2023
D.A. Saravanos, A. Benjeddou, N. Chrysochoidis and T. Theodosiou (Eds)

ACTIVE SHM AND IMPACT SENSING FOR COMPOSITE AEROSPACE STRUCTURES BASED ON THE TEMSAL TECHNOLOGY – DEMONSTRATION ON A GENERIC AIRCRAFT ENGINE CONTAINMENT SEGMENT

Tim Bätzel, Holger Böhm, Andreas Hornig and Maik Gude

Institute of Lightweight Engineering and Polymer Technology (ILK)
Technische Universität Dresden
Holbeinstraße 3, 01307 Dresden, Germany
e-mail: tim.baetzel@tu-dresden.de, web page: http://tu-dresden.de/mw/ilk

Key words: composite, structures, aerospace, aviation, SHM, impact

Abstract. Carbon fibre-reinforced plastic (CFRP) materials are of rising interest for the aerospace and aviation industry in order to achieve objectives towards reduced emissions, resource conservation and cost efficiency. Their typically layered and adaptable material structure offers the possibility to integrate functional elements. Especially electrical units for sensing or actuating can be utilized for structural health monitoring (SHM) applications. The novel Tailored Embeddable Sensor Actuator Layer (TEmSAL) technology for high-performance aerospace composites is utilised to instrument a generic full scale engine containment section with integrated piezo ceramic sensor elements. A tailored sensor network layout based on the structures eigenmodes is developed and aspects of the manufacturing and embedding of the functional element grid are addressed. The results of self-sensing experiments, exploiting the inverse piezoelectric effect in a pitch-catch setup and external excitation test results are presented and discussed. Impact sensing capabilities are explored by exposing the structure to a generic linear fan blade off (LFBO) impact at a velocity of 120 m/s. For this, an innovative setup is developed and discussed, including the impactor and sabot system as well as an adaptable fixture setup to mount the generic containment segment specimen and customize the impact angle. Test results are presented and the sensor performance is discussed.

1 INTRODUCTION

Carbon fibre-reinforced plastic (CFRP) materials are of rising interest for the aerospace and aviation industry in order to achieve objectives towards reduced emissions, resource conservation and cost efficiency. In contrast to metallic materials, CFRPs offer higher specific material properties, such as strengths, stiffness, and an increased energy absorption capacity in case of impact loading scenarios. Moreover, their laminated structure allows for the direct embedding of electrical elements such as sensors and actuators. Thus, composite structures are well suited for application of advanced structural health monitoring (SHM) systems to enable lightweight, cost

Peer-review under responsibility of the organizing committee of SMART 2023.
doi: 10.7712/150123.9802.444217

and resource-efficient structural components and to increase operational safety through real time health monitoring. This approach gains additional relevance when input data for digital twins are required, which is for example addressed by Milanoski et al. in [1]. The primary objective is to enhance the safety and reliability of aerospace vehicles by detecting and diagnosing structural damage, fatigue, and other issues before they become critical.

SHM systems typically use various sensors, such as strain gauges, accelerometers, and temperature sensors, to monitor vehicle structures and detect any changes or anomalies that could indicate potential damage or failure. These sensors can be embedded into the structure of the vehicle or mounted externally, depending on the specific application. Here, lead zirconate titanate (PZT) based sensor/actuator elements are used. They are predestined for an embedded SHM system and impact detection due to their high sensitivity, high temperature stability, relatively low price, high availability and adaptable size. An overview of the applicability of piezoelectric devices has been elaborated by Tuloup et al. in [2].

Aerospace structures are particularly prone to impact loading scenarios, where Soft-Body-Impact (SBI) [3, 4], Foreign-Object-Damage (hail and stone impact, FOD) [5]) and Fan-Blade-Off (FBO) events have to be considered. Aerospace-grade material systems generally involve special requirements to ensure aerospace appropriate performance and safety. Experimental engine containment certification for the case of a catastrophic compressor/turbine blade failure is considered one of the most costly and elaborate test cases since a number of different data acquisition tools and high speed imaging techniques are required and a considerable amount of damage is introduced into the engine system [6]. Tests on most critical compressor and turbine stages are required by the European Union Aviation Safety Agency (EASA) [7]. Thus, accurate testing methods are crucial to ensure the development of a capable design during pre-certification phase. An important tool for the development of such critical structures are simplified testing methods on substructural level. The main objective of simplified FBO testing is to create a setup, which does not require a full containment structure and fan rotor assembly while maintaining a realistic reconstruction of complex impact loads introduced by the release blade. In order to draft and realise a feasible test setup, the two aspects of containment specimen design and test rig design (including impactor setup, acceleration, instrumentation and specimen constraints) have to be considered.

Concerning the integration of electric components in CFRPs, two main challenges arise. Firstly, the influence of embedded systems on the interlaminar behaviour of CFRP composites needs to be assessed [8] and minimized. For this, the usage of polymeric layers has been investigated in detail in [9]. It has been shown that a combined polyimide-polyolefine configuration could be particularly effective as a carrier material for electric components, due to its negligible impact on the interlaminar properties (for the case of integration into epoxy-based CFRP-laminates). Secondly, the inherent electrical conductivity of the carbon fibres in CFRP requires electrical insulation. The Tailored Embeddable Sensor Actuator Layer (TEmSAL) technology has been developed to address these requirements. In [10] it was demonstrated how it can be applied on a structural level by setting up an adapted manufacturing process for generic aerospace fan blade structures. Impact sensing capabilities of the embedded Piezo Ceramic Elements (PCE) were demonstrated using a modal hammer experimental setup and pitch-catch scenarios for self evaluation purposes were investigated. In [4] a methodology is explored to utilize this setup for impact localisation and damage assessment in a SBI setup.

Figure 1: Generic containment segment structure

2 GENERIC ENGINE CONTAINMENT SEGMENT AND FUNCTIONALISATION

The presented study is mainly focused on the use case of a generic engine containment for testing on Technology Readiness Level (TRL) 3. In order to establish a simplified test setup for low overhead testing of new concepts (detailed description in Sec. 4), the structure is reduced to a segment of approximately 51.4 ° arc angle (1/7 of the full structure) with an arc length of 420 mm and a height of 240 mm. Flanges for bolt connections are included at the outer edges in circumferential direction. The resulting specimen geometry is illustrated by Fig. 1.

An aerospace-grade prepreg CFRP with epoxy matrix material and unidirectional carbon fibre reinforcement (CYCOM™ 977-2) was used. The manufacturing of this material requires a high temperature autoclave curing process up to T_c =180 °C and a pressure of p_c =7 bar for consolidation.

Functionalisation of the generic containment segment structure was achieved through the application of TEmSAL [10]. These functional layers are based on Polyimide (PI) carrier foils with screen printed conductive tracks, integrated PCEs and contact terminals for wire connection at the outer edge of the host structure. The following requirements for the functional layers can be derived from the presented use case scenario of an impact loaded containment structure:

- conservation of high mechanical laminate properties (minimisation of disturbance by functional layer);
- electrical insulation (carbon fibre to functional elements);
- high temperature stability of all components to withstand consolidation process;
- high signal to noise ratio for robust data acquisition;
- adaptable sensor layout to enable tailored solutions for individual structures;
- reliable electrical contacting at the structures interface.

Sufficient temperature stability of TEmSAL was achieved through the implementation of high temperature suitable materials only (PI foils and ceramic based active material). Reliable

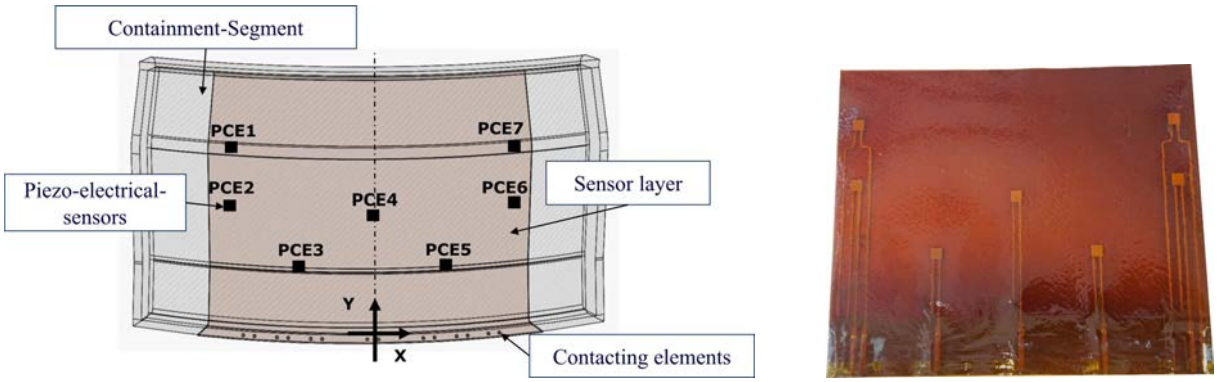

(a) Sensor positions with coordinate system

(b) TEmSAL prior integration

Figure 2: Overview of TEmSAL tailored for the containment structure

Table 1: Sensor coordinates for the corresponding coordinate system in Fig. 2a

identifier	PCE1	PCE2	PCE3	PCE4	PCE5	PCE6	PCE7
x-coordinate	-125	-127	-66	0	66	127	125
y-coordinate	151	99	40	87	40	99	151

electrical insulation was ensured by a continuous PI carrier foil enclosure of all electric components. The continuous PI layer of TEmSAL poses a potential discontinuity, weakening the host structure's laminate. However, it was demonstrated by Hornig et al. [9] that the used PI material in combination with an additional polyolefine layer acting as adhesion promoter allows for a high interlaminar fracture toughness. Thus, the TEmSAL-CFRP interface is not prone to premature failure through delamination. High sensitivity to mechanical deformation was achieved through the implementation of PZT based PCEs and reliable electrical contacting was enabled through brass tube based contact terminals [10]. The screen printing process for application of conductive tracks to the carrier foils allows for the creation of a sensor network layout tailored to the surrounding host structure.

A sensor network layout for the presented generic containment structure was developed by analysing the structures first eight eigenmodes. Areas of high strain for those eigenmodes were chosen as sensor positions, ensuring high signal to noise ratios. Resulting sensor positions and TEmSAL layout are illustrated by Fig. 2 and Tab. 1.

The functional layer was integrated during preforming. The preforming process itself was performed on the same one sided mould used for autoclave consolidation (Fig. 3a). A layup sequence of $[0_2/+45_2/90_2/-45_2/0_2/+45_2/90_2/-45_2/0_2/90]_s$ was chosen in order to avoid high differences in fibre orientation of adjecent plies and, thus, to minimise delamination tendency during impact loading. The functional layer was inserted between second and third ply close to the back surface of the structure (non impacted surface), see Fig. 3c.

After preforming was completed, the mould was prepared for consolidation (including vacuum bagging) and the consolidation process was started The final steps of manufacturing were demoulding and trimming of the outer edges. Through precise milling, all excess material was

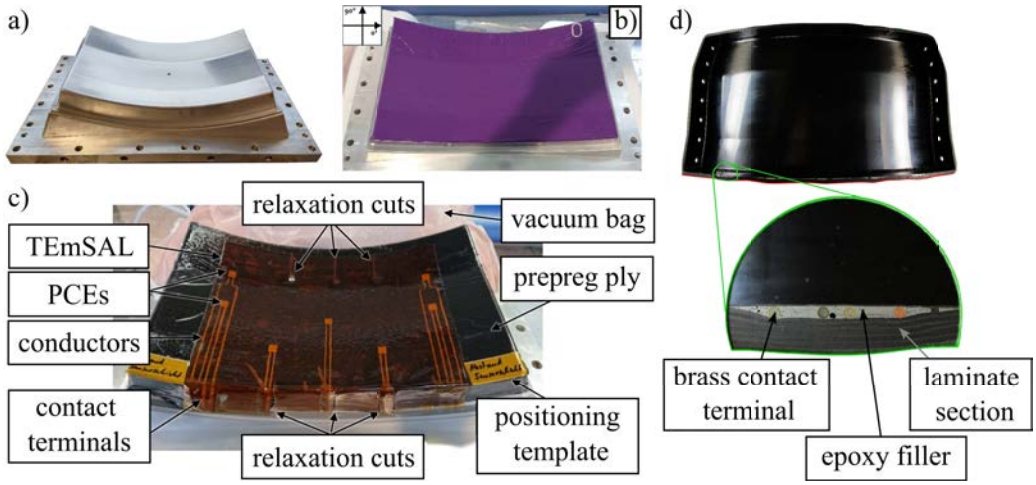

Figure 3: Manufacturing of generic containment specimen with a) mould; b) Prepreg plies applied to mould during preforming; c) Integration of TEmSAL during preforming and d) generic containment structure with uncovered contact terminals

removed and the contact terminal were uncovered (Fig. 3d). Two containment segments with identifiers CO-1 and CO-2 were manufactured.

3 FUNCTIONAL TESTING AND SELF SENSING

Prior to Linear Fan-Blade-Off (LFBO) testing, a number of non-destructive functional tests including self excitation (pitch-catch setup) on containment segment CO-2 and external excitation via instrumented impact hammer on containment segment CO-1 were conducted. Those tests contributed to the verification of functionality as well as the collection of data on the structures modal characteristic and functional system sensitivity.

3.1 External excitation

For the first functional test, an instrumented impact hammer was used as external excitation source to introduce oscillations into the structure (CO-1). During this procedure, the structure was mounted on a fixture simulating in-service installation conditions. This test rig was also used for linear fan blade off testing and is elaborated in Sec. 4. Signals were recorded using a NI 5105 digitiser (National Instruments Corp.), see Fig. 4. The overall setup was similar to external excitation experiments presented in Hornig et al. [10]. Resultant signals (Fig. 4b and Fig. 4c) indicated that PCE2 and PCE3 were damaged during manufacturing as only noise was recorded for those PCEs. In contrast, distinctive signals with amplitudes well above noise levels could be obtained from PCE1,4-7 for the comparably low impulse introduced into the high stiffness containment structure. Those findings confirm that the TEmSAL system is suitable to detect even low magnitude operational loads.

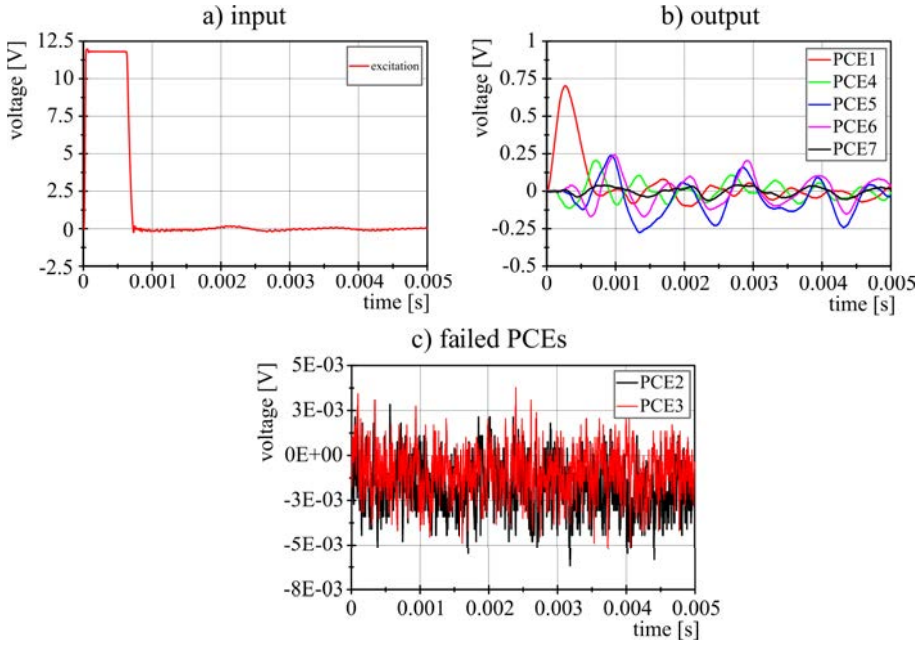

Figure 4: Signal waveforms obtained from external excitation testing with a) Waveform of introduced impuls, b) Signals recovered by integrated PCEs (functional) and c) Signals of damaged PCEs

3.2 Self excitation

Following the external excitation test, a self sensing test in pitch-catch configuration was conducted on containment segment CO-2 to demonstrate and validate the TEmSAL systems ability to fulfill active condition monitoring tasks through using the integrated PCEs in both, actuator and sensor mode. For the self excitation test, the structure was constrained by the same boundary conditions used for external excitation testing. PCE4 was used as excitation source. A sinusoidal voltage signal with a frequency of 2 kHz and an amplitude of 175 V was used as input, exploiting the inverse piezo-electric effect to generate defined oscillations (Fig. 5a). The waveform was generated using a NI 5406 waveform generator (National Instruments Corp.). Resultant signals were captured using a NI 5105 digitiser (National Instruments Corp.).

Throughout the experiment it was concluded, that PCE3 and PCE7 were damaged during manufacturing (only noise was recovered from the recordings). PCE1, PCE5 and PCE6 (Fig. 5b) recovered the distinctive input waveform with signal levels well above the noise level. Amplitudes were in the range of 0.7 V to 1.7 V with a slight phase shift between single PCEs. However, PCE2 (Fig. 5c) produced only low amplitude outputs in the range of 3 mV, which are significantly disturbed by the present electromagnetic interference. The signal in Fig. 5c was already smoothed by a moving average filter, still showing significant disturbances.

4 LINEAR FAN BLADE OFF TESTING

The presented LFBO setup utilises a compressed air gun (gas gun) with a barrel diameter of 80 mm for linear acceleration of a fan blade fragment impactor. The basic gas gun setup is

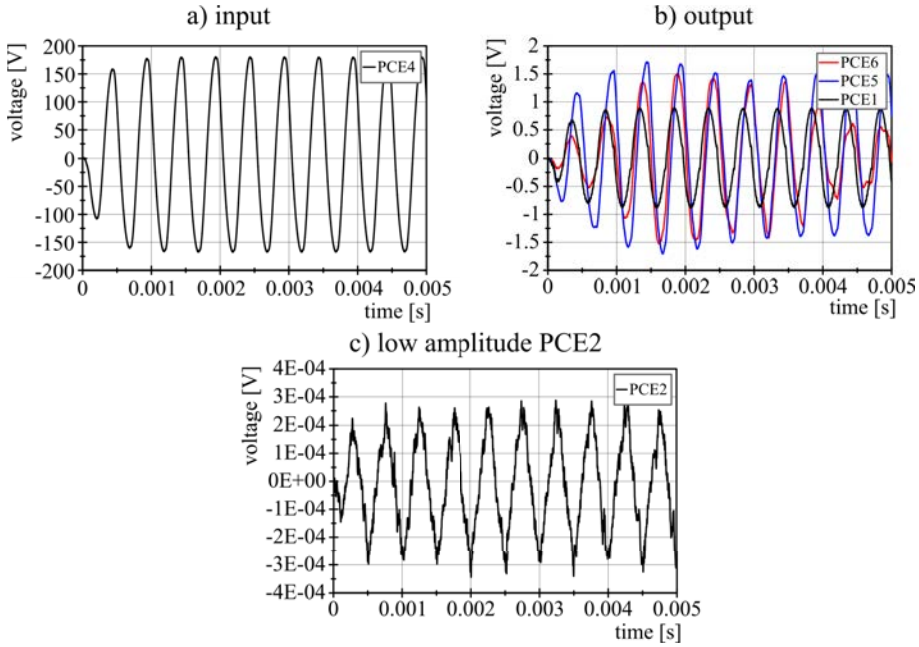

Figure 5: Signal waveforms obtained from internal excitation testing with a) Excitation waveform of PCE4, b) Signals recovered by integrated PCEs (functional) and c) Low amplitude signal of PCE2

presented in [3], where it has been used for SBI experiments. In the current study, a static containment section specimen assembly positioned at a defined impact angle is impacted after a linear acceleration phase. The target impact velocity was 120 m/s. This test rig concept is set to eliminate the need for highly complex rotor test beds during early development testing of containment structures (approx. at TRL3) enhancing cost and time efficiency.

4.1 Specimen fixture

Main requirements for the design of a suitable specimen fixture was to ensure a high level of adjustability as well as realistic boundary conditions to simulate the in-service installation conditions. Both connection flanges of the containment segment are bolted to rigid steel plates. An angle of 36 ° between the impactor trajectory and containment segment normal vector at the impact location was set. Angular adjustability was achieved using a bolt connection with slotted holes. The impact center position was set to the geometrical center of the containment segment (x=0 mm and y=120 mm according to the coordinate system in Fig. 2a). The integrated PCEs were connected to a NI 5105 digitiser (National Instruments Corp.) for data acquisition during impact.

4.2 Impactor and sabot system

Impactor size was limited by the available gas gun barrel diameter of 80 mm. Thus, a laminated CFRP blade strip impactor of 60 mm in width and a length of 304 mm was designed (Fig. 7c). The impactor design features a conical cross-section with a linear increasing thickness

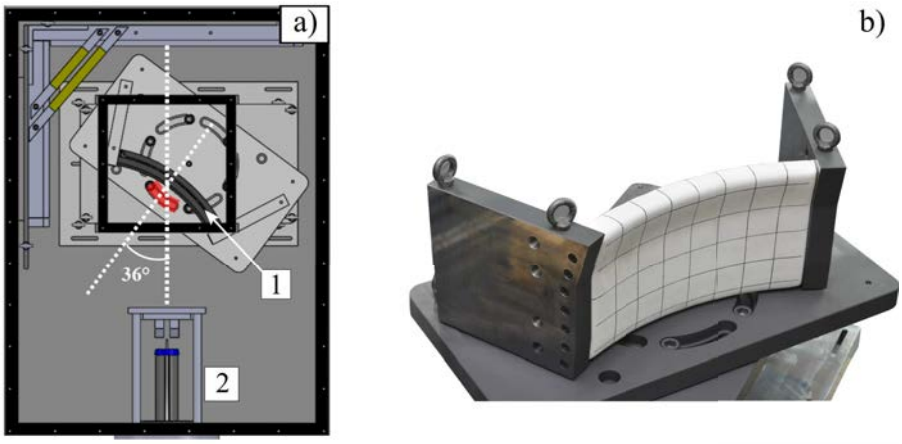

Figure 6: a) Test setup position in relation to the gas gun muzzle (1: generic containment segment specimen; 2: gas gun muzzle); b) Picture of specimen fixture with containment segment

of 5 mm at the front end (tip) and 12 mm at the rear end (root). The layup was composed of 67 layers of CYCOM™ 977-2 (same material as containment structure) at the root. Adapted sizing of plies was used to create the conical cross-section. The layup sequence was chosen to be similar to typical fan blade layups. In order to achieve reproducible impact conditions, a custom sabot system consisting of 3D printed endcaps (Fig. 7a) and polymer spacer shells (Fig. 7b) was developed. The endcaps ensured a stable positioning of the impactor during acceleration in the barrel using the barrel guiding rail (Fig. 7d). Further, the barrel was sealed by the endcaps to allow pressure buildup behind the projectile assembly and enabling acceleration. Spacer shells were set up to connect and stabilise both endcaps.

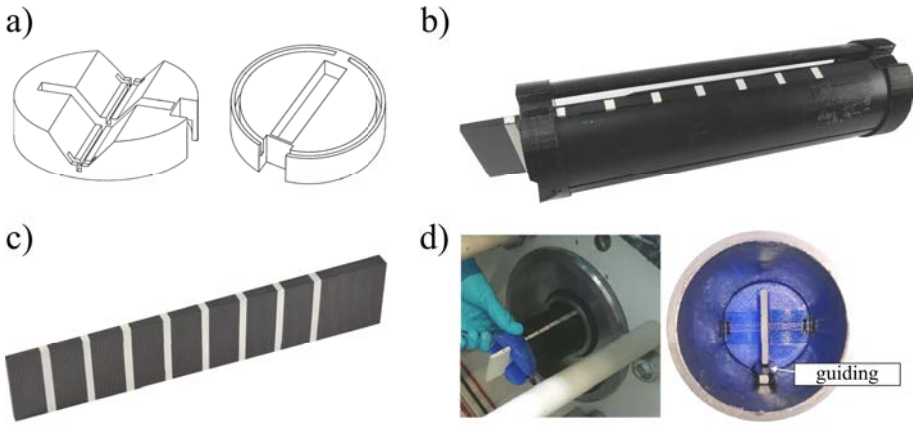

Figure 7: Projectile setup with a) 3D printed endcaps; b) Projectile assembly; c) Laminated CFRP impactor and d) Projectile assembly in gas gun barrel

After accelerating the Sabot containing the impactor in the barrel it exits the outlet and enters the free flight phase. During this phase and prior to impact, the sabot assembly has to be

separated from the impactor itself. For this purpose, a sabot stripper in splitter configuration was designed and implemented (Fig. 8). A commissioning test without target structure was conducted to verify sabot stripper system feasibility. As seen in Fig. 8b, the sabot is fully separated without disturbing the impactor flight trajectory.

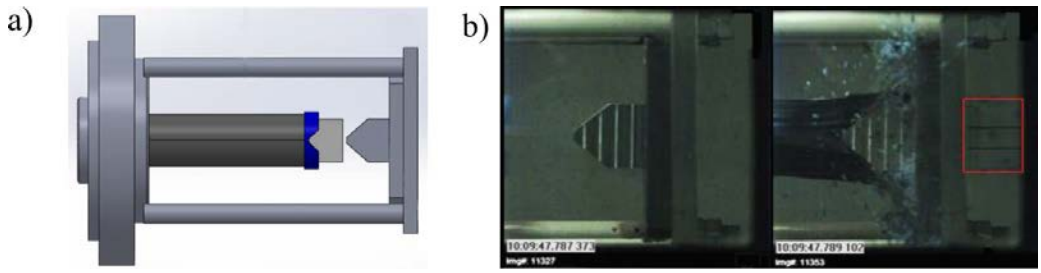

Figure 8: a) Sabot stripper system and b) commissioning test for verification of sabot stripper design (impactor passing the sabot stripper marked red)

4.3 Results

High speed imaging footage of the conducted LFBO is presented in Fig. 9. Camera 1 captured the frontal view of the impact while camera 2 captured the top view. The blade strip impactor was deflected at impact and slid along the containment segment surface. No visible impact damage was introduced to the structure while the blade strip impactor was fragmented due to severe delamination failure.

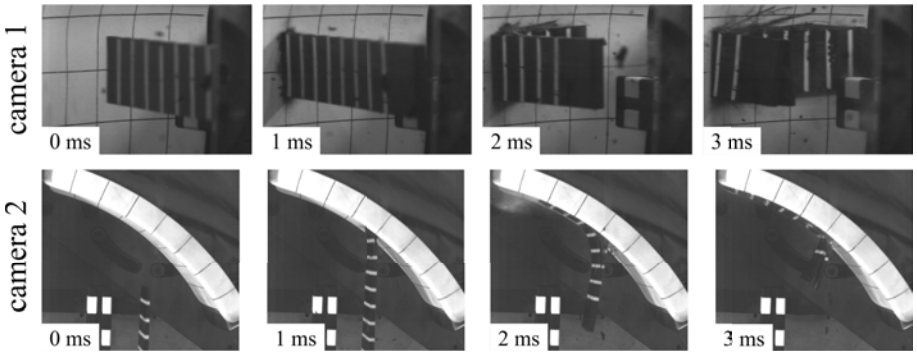

Figure 9: High speed camera footage of top and frontal view during LFBO

Post impact ultrasonic transmission measurements revealed three visible echos (A-C in Fig. 10). Those echos are attributed to delamination formation in the areas of PCEs 2, 4 and 6, which impose an inhomogeneity for the transmission of ultrasonic waves. Delamination in the areas of PCE2 and PCE6 (A and C in Fig. 10) were classified as minor damages at the PCE edge areas, since the echos are roughly the size of the integrated PCEs. However, a delamination of 44 mm by 34 mm was measured directly at the impact position center around PCE4 (B in Fig. 10).

The LFBO was conducted on containment segment CO-1 (PCE2 and PCE3 non-functional). During testing PCE4 failed due to severe damage and PCE1 did not retrieve a usable signal

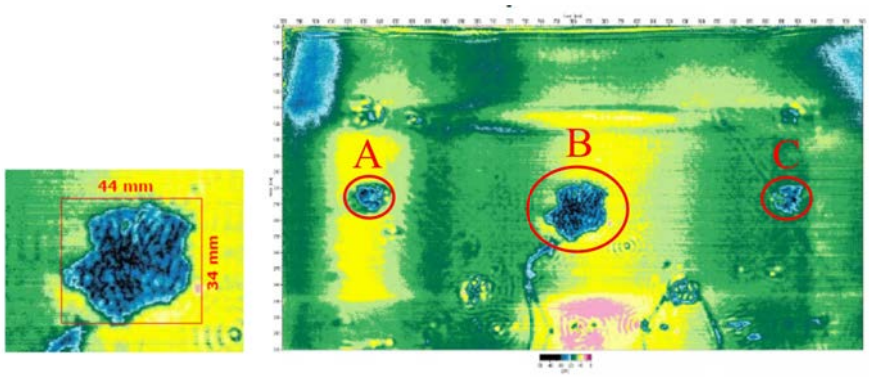

Figure 10: Post impact ultrasonic transmission plot with three visible echos in the areas of PCE2 (A), PCE4 (B) and PCE6 (C) due to delamination

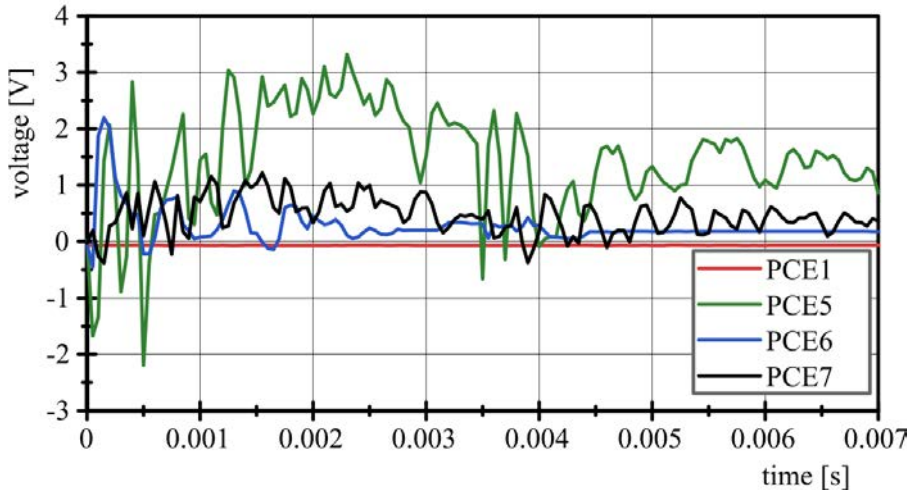

Figure 11: PCE signals of the LFBO at 120 m/s

due to failure of contacting (plotted in Fig. 11). The signals received by PCE5-7 are plotted in Fig. 11. The measurement circuits were modified to achieve a signal down scaling by the factor of 20 compared to the results of external and internal excitation tests. Through this, the data acquisition equipment (NI 5105 digitiser) was protected from high voltages generated by the PCEs during impact. From the signal time series it is apparent that shock loading with severe oscillations is introduced by the initial impact of the blade tip (0-0.5 ms) followed by a phase of higher signal output of PCE5 and PCE7 (1-3 ms). This high output phase is attributed to the blade sliding over the containment surface towards PCE5-7. At the time stamp of 4 ms, the loading process is finished. PCE5 retained an irreversible signal component of approximately 1.4 V. Overall, the resulting maximum signal value was 3.3 V for PCE5.

5 CONCLUSION

The TEmSAL technology was successfully applied to a complex curved containment segment structure. All requirements resulting from the application of high performance aerospace-grade CFRP materials were addressed and fulfilled. Active and passive sensing capabilities of TEmSAL were demonstrated in a pitch-catch setup as well as in an impact hammer excitation setup. Through the obtained results it was proofed, that the sensoric system sensitivity of TEmSAL is high enough to capture oscillation caused by low intensity excitations. Especially, the actuation intensity threshold of the PCE material (mainly limited by the PCEs upper voltage limit) is high enough to produce oscillations that can be detected sufficiently by other PCEs in sensoric operation mode. Thus, TEmSAL is suitable to implement an active condition and health monitoring system for structures of comparable size.

The setup developed for LFBO testing is capable of reproducing the release blade behavior and main impact conditions on the containment (as seen on high speed camera footage). This proofs the LFBO test configuration as a useful tool to de-risk containment tests, allow for low overhead fan blade off testing and provide valuable high quality validation data for numerical modelling along the development process.

However, further improvement of processing parameters for the manufacturing of the TEmSAL itself and the integration process are necessary to minimise sensor failure during integration and achieve consistent high quality. The utilisation of a larger gas gun barrel would enable the inclusion of a full blade root with dove tail. Thus, effects of root impacts on the containment could also be considered.

ACKNOWLEDGMENT

The authors wish to acknowledge the support of Rolls-Royce plc through the Lightweight Structures and Materials and Robust Design UTC at the Technische Universität Dresden. The results are also partially based upon work from COST Action HISTRATE (Composites under HIgh STRAin raTEs loading: a route to certification-by-analysis), CA21155, supported by COST (European Cooperation in Science and Technology).

REFERENCES

[1] D. Milanoski, G. Galanopoulos, D. Zarouchas, and T. H. Loutas, "Multi-level damage diagnosis on stiffened composite panels based on a damage-uninformative digital twin," *Structural Health Monitoring*, vol. 22, pp. 1437 – 1459, 2022. [Online]. Available: https://doi.org/10.1177/14759217221108676

[2] C. Tuloup, W. Harizi, Z. Aboura, Y. Meyer, K. Khellil, and R. Lachat, "On the manufacturing, integration, and wiring techniques of in situ piezoelectric devices for the manufacturing and structural health monitoring of polymer–matrix composites: A literature review," *Journal of Intelligent Material Systems and Structures*, vol. 30, no. 16, pp. 2351–2381, 2019. [Online]. Available: https://doi.org/10.1177/1045389X19861782

[3] A. Cochrane, J. Serra, J. Lander, I. Partridge, H. Böhm, T. Wollmann, A. Hornig, M. Gude, and S. Hallett, "Experimental investigation of large-scale high-velocity soft-body

impact on composite laminates," *International Journal of Impact Engineering*, vol. 161, p. 104089, 2022. [Online]. Available: https://doi.org/10.1016/j.ijimpeng.2021.104089

[4] S. Cuomo, T. Bätzel, N. Modler, A. Hornig, and M. Meo, "High velocity impact on generic cfrp blade specimen: baseline free method for impact localisation and damage assessment on complex structures," *Smart Mater. Struct.*, vol. 31, 2022. [Online]. Available: https://doi.org/10.1088/1361-665X/ac6d90

[5] H. Böhm, L. Högner, M. Meyer, R. Mailach, A. Hornig, and M. Gude, "A Methodology for a Coupled Structural–Computational Fluid Dynamics Analysis of Compressor Rotor Blades Subjected to Ice Impact With Uncertain Impactor Parameters," *Journal of Engineering for Gas Turbines and Power*, vol. 145, no. 3, 12 2022, 031001. [Online]. Available: https://doi.org/10.1115/1.4055687

[6] B. Yang, "Blade containment evaluation of civil aircraft engines," *Chinese Journal of Aeronautics*, vol. 26, no. 1, pp. 9–16, feb 2013. [Online]. Available: https://doi.org/10.1016/j.cja.2012.12.001

[7] *Certification Specifications and Acceptable Means of Compliance for Engines (CS-E)*, EASA, Jun. 2020.

[8] S. Butler, M. R. Gurvich, A. Ghoshal, G. Welsh, P. Attridge, H. A. Winston, M. R. Urban, and N. E. Bordick, "Effect of embedded sensors on interlaminar damage in composite structures," *Journal of Intelligent Material Systems and Structures*, vol. 22, pp. 1857 – 1868, 2011. [Online]. Available: https://doi.org/10.1177/1045389X11414225

[9] A. Hornig, A. Winkler, E. Bauerfeind, M. Gude, and N. Modler, "Delamination behaviour of embedded polymeric sensor and actuator carrier layers in epoxy based cfrp laminates—a study of energy release rates," *Polymers*, vol. 13, no. 22, 2021. [Online]. Available: https://doi.org/10.3390/polym13223926

[10] A. Hornig, R. Frohberg, T. Bätzel, M. Gude, and N. Modler, "Embedded sensing and actuating in CFRP composite structures—concept and technology demonstration for tailored embeddable sensor-actuator layers (TEmSAL)," *Smart Materials and Structures*, vol. 31, no. 9, p. 095007, jul 2022. [Online]. Available: https://doi.org/10.1088/1361-665X/ac7d23